

# E-Selectin Up-Regulation Allows for Targeted Drug Delivery in Prostate Cancer<sup>1</sup>

Vinay Bhaskar, Debbie A. Law, Eric Ibsen, Danna Breinberg, Kellie M. Cass,<sup>2</sup> Robert B. DuBridg, Ferdinand Evangelista, Susan M. Henshall, Peter Hevezi,<sup>3</sup> Jennifer C. Miller, Melody Pong, Rick Powers, Peter Senter, David Stockett, Robert L. Sutherland, Ursula von Freeden-Jeffry, Dorian Willhite,<sup>3</sup> Richard Murray, Daniel E. H. Afar, and Vanitha Ramakrishnan<sup>4</sup>

Protein Design Labs, Inc., Fremont, California 94555 [V. B., D. A. L., E. I., D. B., R. B. D., F. E., J. C. M., M. P., R. P., U. v. F.-J., R. M., D. E. H. A., V. R.]; Garvan Institute of Medical Research, St. Vincent's Hospital, Darlinghurst, Sydney, NSW 2010, Australia [S. M. H., R. L. S.]; Seattle Genetics, Inc., Bothell, Washington 98021 [P. S.]; and Eos Biotechnology, Inc., South San Francisco, California 94080 [K. M. C., P. H., D. S., D. W.]

## ABSTRACT

We have used the Eos Hu03 GeneChip array, which represents over 92% of the transcribed human genome, to measure gene expression in a panel of normal and diseased human tissues. This analysis revealed that E-selectin mRNA is selectively overexpressed in prostate cancer epithelium, a finding that correlated strongly with E-selectin protein expression as assessed by immunohistochemistry. Antibodies against E-selectin that blocked function failed to impede cancer cell growth, suggesting that overexpression of E-selectin was not essential for cell growth. However, a novel auristatin E-based antibody drug conjugate (ADC), E-selectin antibody valine-citrulline monomethyl-auristatin E, was a potent and selective agent against E-selectin-expressing cancer cell lines *in vitro*, with the degree of cytotoxicity varying with surface antigen density. Interestingly, sensitivity to the ADC differed among cell lines from different tissues expressing similar amounts of E-selectin and was found to correlate with sensitivity to free auristatin E. Furthermore, E-selectin-expressing tumors grown as xenografts in severe combined immunodeficient mice were responsive to treatment with E-selectin antibody valine-citrulline monomethyl-auristatin E *in vivo*, with more than 85% inhibition of tumor growth observed in treated mice. These findings demonstrate that an E-selectin-targeting ADC has potential as a prostate cancer therapy and validates a genomics-based paradigm for the identification of cancer-specific antigens suitable for targeted therapy.

## INTRODUCTION

Prostate cancer, the fourth most frequently diagnosed cancer in men, has an annual mortality rate of 40,000 in the United States alone. Treatment of locally confined prostate cancer, consisting of radical prostatectomy and/or radiotherapy, is often associated with undesirable side effects such as impotence and urinary incontinence. In addition, 30% of patients develop recurrent and metastatic disease, which is essentially untreatable (1). Thus, the identification of novel, effective therapeutic targets in prostate cancer is critical for improving disease treatment and management, thereby increasing survival.

Recent therapeutic success in the cancer arena has been achieved by the use of mAbs<sup>5</sup> that target molecules selectively up-regulated on the

surface of tumor cells (e.g., HER2 in breast cancer). Accordingly, an ideal target for prostate cancer therapy would be highly expressed in diseased tissue with minimal expression in other body tissues. To identify prostate cancer-specific antigens, genome-wide transcript profiling was applied to prostate cancer tissues and a broad panel of distinct normal body tissues. Comprehensive bioinformatics analysis was used to identify genes encoding known or predicted cell surface molecules with specific or enriched expression in the prostate cancer samples. A number of cell surface molecules were subsequently identified as prostate cancer tumor antigens, one of which was E-selectin.

E-selectin, also known as endothelial adhesion molecule 1 (ELAM-1, CD62E), is a type Ia transmembrane protein containing lectin-like and endothelial growth factor-like domains, followed by short cysteine-rich repeats (2). Absent in resting epithelium, E-selectin is rapidly expressed in the vascular lining during inflammation (3). Indeed, activation of endothelial cells by proinflammatory cytokines results in the cell surface appearance of E-selectin, facilitating leukocyte rolling and extravasation through activated endothelium (4, 5). The up-regulation of E-selectin in prostate cancer, together with its limited expression in normal body tissues, makes it a potential target for therapeutic mAbs that are intended to destroy target cells.

In this study, we test the use of E-selectin as a therapeutic target by using auristatin E-conjugated anti-E-selectin-specific mAbs. Auristatin E belongs to the dolastatin 10 family of cytotoxic agents, potent inhibitors of microtubule polymerization that cause significant apoptosis in a variety of cell culture and xenograft models (6–8). Our data demonstrate that toxin-conjugated anti-E-selectin mAbs exhibit specific cytotoxicity to E-selectin-expressing cancer cells *in vitro* and *in vivo*. These results indicate that E-selectin is a potential therapeutic target for the treatment of cancers that exhibit up-regulated expression of this protein.

## MATERIALS AND METHODS

**Transcript Profiling.** Fresh-frozen tissue from 74 patients treated with radical prostatectomy for clinically localized prostate cancer was collected at St. Vincent's Hospital (Sydney, Australia) between 1996 and 2000 (median follow-up, 28.3 months; range, 4.9–95.2; Ref. 9). Each sample chosen for RNA preparation was identified by a pathologist as tumor tissue. Table 1 summarizes the clinical data for the patient samples. Over 200 normal adult tissues representing 43 different body tissues were also collected. Total RNA was extracted from specimens with Trizol reagent (Invitrogen) and reverse transcribed using a primer containing oligo(dT) and a T7 promoter sequence. Resulting cDNAs were transcribed *in vitro* in the presence of biotinylated nucleotides (Bio-11-CTP and Bio-16-UTP) using the T7 MEGAscript kit (Ambion) and hybridized to the Eos Hu03 expression array, a customized Affymetrix GeneChip array containing over 59,000 probe sets for the interrogation of over 46,000 genes, EST clusters, and predicted exons based on the first draft of the human genome as described previously (10).

**Plasmid Construction.** The vector pNEF5 (ICOS Corporation) was modified at its unique *Xba*I site to include a *Pac*I cloning site, followed by an *Xho*I site, a COOH-terminal HA tag, and the human Ig heavy chain polyA sequence.

Received 4/7/03; revised 6/13/03; accepted 7/21/03.

The costs of publication of this article were defrayed in part by the payment of page charges. This article must therefore be hereby marked *advertisement* in accordance with 18 U.S.C. Section 1734 solely to indicate this fact.

<sup>1</sup> Supported in part by grants from the National Health and Medical Research Council of Australia (to R. L. S.), the Prostate Cancer Foundation of Australia (to S. M. H.), and The Cancer Council New South Wales (to S. M. H. and R. L. S.).

<sup>2</sup> Present address: AGY Therapeutics, Inc., 290 Utah Avenue, South San Francisco, California 94080.

<sup>3</sup> Present address: Neurocrine Biosciences, Inc., 10555 Science Center Drive, San Diego, California 92121.

<sup>4</sup> To whom requests for reprints should be addressed, at Protein Design Labs, Inc., 34801 Campus Drive, Fremont, CA 94555. Phone: (510) 742-2852; Fax: (650) 574-1500; E-mail: vramakrishnan@pdl.com.

<sup>5</sup> The abbreviations used are: mAb, monoclonal antibody; ADC, antibody drug conjugate; AIU, average intensity unit(s); E-sel-VC-MMAE, E-selectin antibody valine-citrulline monomethyl-auristatin E conjugate; TNF- $\alpha$ , tumor necrosis factor  $\alpha$ ; HUVEC, human umbilical vein endothelial cell; IMDM, Iscove's modified Dulbecco's medium; FBS, fetal bovine serum; SCID, severe combined immunodeficient; FACS, fluorescence-activated cell sorter; PSCA, prostate stem cell antigen; MFI, mean fluorescence intensity; HA, hemagglutinin.

Table 1 Patient clinical data

Patient no. <sup>a</sup>	E-selectin level <sup>b</sup>	Pathological stage	Gleason score	PSA <sup>c</sup>
1	121	PT3A	7	6.4
2	46	PT2C	7	9.3
3	124	PT3B	7	11
4	101	PT2A	6	3.2
5	59	PT2C	6	7.7
6	145	PT2A	7	4.8
7	90	PT2C	7	7.6
8	51	PT3A	7	28.3
9	18	PT2C	6	4
10	63	PT2C	6	5.9
11	63	PT2B	7	6.3
12	84	PT3C	7	6.2
13	103	PT2C	7	4.5
14	142	PT4A	7	7.8
15	27	PT2C	7	4.7
16	-11	PT2B	8	8.1
17	188	PT2C	6	9.6
18	104	PT3A	7	10.5
19	14	PT3A	9	16
20	-65	PT3A	7	3.8
21	98	PT3C	8	9.1
22	-5	PT3C	9	9.5
23	195	PT3A	7	10.3
24	1	PT3A	6	9.4
25	87	PT3C	7	12.3
26	150	PT2C	7	5.7
27	153	PT3B	7	15
28	318	PT4A	7	13.2
29	0	PT3C	7	16.5
30	92	PT3A	7	12.4
31	-70	PT3A	7	6.3
32	109	PT3C	6	8.2
33	55	PT3C	7	7
34	117	PT3A	7	12
35	261	PT4A	7	7.1
36	323	PT4A	7	23.8
37	38	PT2C	6	6.5
38	-3	PT2C	7	12
39	41	PT3B	8	3.6
40	-41	PT3A	7	15
41	89	PT3A	7	9
42	-74	PT3C	7	21.6
43	-45	PT3A	7	10.3
44	-58	PT3A	9	3.1
45	171	PT3A	7	19.6
46	170	PT2B	9	11.5
47	48	PT4A	7	14.3
48	-36	PT3A	7	7
49	235	PT3B	7	20.3
50	96	PT2B	6	8.2
51	-24	PT3C	9	11.8
52	24	PT2C	7	23.9
53	167	PT3C	8	15
54	225	PT2A	7	12
55	48	PT3C	7	20
56	81	PT2C	7	17.1
57	-10	PT3A	6	6.7
58	201	PT3C	7	50.4
59	-20	PT3A	7	32.6
60	41	PT3C	7	5.9
61	-72	PT3B	7	6.9
62	-82	PT3C	9	4.9
63	-2	PT3A	6	6.6
64	-92	PT4B	8	7.1
65	118	PT3B	7	6.9
66	50	PT2B	7	8.59
67	114	PT3A	7	5.8
68	-65	PT3A	7	15.9
69	374	PT3A	7	10.3
70	28	PT2B	6	5
71	292	PT2C	6	7.3
72	324	PT2C	7	5.8
73	-30	PT3A	6	20.8
74	10	PT3A	7	8

<sup>a</sup> As listed in Fig. 1.

<sup>b</sup> AIU as determined on Eos Hu03 GeneChip array.

<sup>c</sup> PSA, prostate-specific antigen.

This vector, pNEF5-HA, was digested with *PacI* and *XhoI* and gel purified. A fragment containing the complete E-selectin protein coding sequence, amplified by PCR from a HUVEC cDNA library, was similarly purified, and the two fragments were ligated overnight using T4 DNA ligase. This reaction was

transformed into Top10 competent cells (Invitrogen), and insert-containing vectors (pNEF-HA-Esel) were identified by gel electrophoresis.

**Cell Culture and Transfections.** All tissue culture reagents were obtained from Invitrogen, unless otherwise noted. HUVECs were obtained from Cascade Biologics and cultured as per the manufacturer's instructions. HCT116, Calu6, and PC3 cells were obtained from American Type Culture Collection and maintained in IMDM, McCoy's medium, or DMEM, respectively, containing 10% FBS (Hyclone) and supplements. For the establishment of stable cell lines, monolayers were transfected with pNEF-HA-Esel or pNEF-HA vector (4  $\mu$ g) and Lipofectamine 2000 reagent (12  $\mu$ l; Invitrogen) in 6-well plates as per the manufacturer's instructions, selected in medium containing G418 (500  $\mu$ g/ml), and cloned by limiting dilution. Clones were screened for E-selectin expression by flow cytometry, expanded, and maintained in G418-containing medium.

**Immunohistochemistry.** Frozen prostate tissue samples (Trigenics), or tumor xenografts from transfected HCT116 colon carcinoma cells grown s.c. in CB-17 SCID mice, were frozen in OCT compound and stored at  $-70^{\circ}\text{C}$ . Cryostat tissue sections (7  $\mu$ m) were fixed in 75% acetone/25% ethanol for 1 min. Twelve prostate cancer tissue sections ranging from Gleason score 4 to 8 were stained. Samples were incubated with either E-selectin-specific mAb 5D11 (5  $\mu$ g/ml; R&D Systems) or control mouse IgG1 [TIB191, a mouse antitrinitrophenol mAb (hybridoma clone 1B76.11; American Type Culture Collection)] for 30 min. Antibody binding was detected using biotinylated secondary antibody [Goat antimouse IgG (3  $\mu$ g/ml, 30 min; Jackson ImmunoResearch)] and developed using the Vectastain Elite ABC kit (Vector Laboratories) and stable diaminobenzidine and  $\text{H}_2\text{O}_2$  (Research Genetics). Staining was performed using the DAKO Autostainer at room temperature.

**ADC Chemistry.** An E-sel-VC-MMAE ADC was prepared as described previously (6). In brief, purified 5D11 (a function/adhesion blocking antibody, as defined by R&D Systems) or TIB191 was reduced with 10 mM DTT, and thiol content was determined by measuring  $A_{412}$  after incubation with Ellman's reagent and subsequent calculation. Equimolar maleimide-VC-MMAE solution [8 mM in DMSO (Sigma)] in cold acetonitrile (20% final concentration) was incubated with reduced mAb for 30 min at  $4^{\circ}\text{C}$ . Unconjugated VC-MMAE was removed by dialysis at  $4^{\circ}\text{C}$  into PBS and filtered. Conjugated mAb was quantified using  $A_{280}/A_{260}$ , and the extent of aggregate *versus* monomer was determined by size-exclusion high-performance liquid chromatography. Finally, matrix assisted laser desorption ionization-time of flight mass spectrometry was used to determine the number of drug molecules per mAb.

**Flow Cytometry.** Cells were removed with 5 mM EDTA in Tris-HCl (pH 8.0) and blocked by centrifugation in HBSS containing 3% heat-inactivated FBS, 1% normal goat serum (Sigma), and 1% BSA at  $4^{\circ}\text{C}$  for 5 min. Cells were incubated for 1 h at  $4^{\circ}\text{C}$  with anti-E-selectin-FITC (10  $\mu$ g/ml; R&D Systems) in FACS buffer (PBS containing 0.1% BSA). Excess mAb was removed by centrifugation, and cells were resuspended in FACS buffer containing propidium iodide (1  $\mu$ g/ml). Fluorescence intensity was measured on a FACScan (Becton Dickinson). Quantitative FACS was performed in a similar manner, except that a saturating concentration of anti-E-selectin-FITC (50  $\mu$ g/ml) was used on cells and similarly treated Quantum Simply Cellular beads (Sigma), a mixture of four populations of agarose beads of known antibody binding content. Antibody binding site quantification was performed by comparing the MFI of each cell line with that of the Quantum Simply Cellular bead populations and correcting for nonspecific effects, as described (11, 12). Experiments were performed twice in triplicate.

**Immunofluorescence.** HCT116 cells grown on coverslips were chilled on ice in growth medium for 10 min. Growth medium was replaced with medium containing 5D11 (10  $\mu$ g/ml) at  $4^{\circ}\text{C}$  for 1 h. Antibody binding was detected using AlexaFluor-488 goat antimouse secondary antibody (1:2200 dilution in chilled growth media; Molecular Probes). Cells were washed three times with PBS, fixed using 5% UltraPure Formaldehyde in PBS for 40 min and washed two additional times using PBS. Slides were mounted using Permafluor (Coulter) for visualization.

**In Vitro Growth Assays.** HCT116, Calu6, and PC3 cell lines were plated at a density of 2500 cells/well in 96-well plates and allowed to recover overnight in phenol red-free IMDM containing 10% FBS and supplements (growth medium). Cells were challenged for 1 h with mAb or ADC (twice in a volume of 50  $\mu$ l) in IMDM at the indicated concentrations. Cells were then washed twice with growth medium and allowed to proliferate in fresh growth medium for 4 days, then cell viability was assessed by the CellTiter 96

Aqueous Non-Radioactive Cell Proliferation Assay (Promega), as per the manufacturer's instructions. HUVECs were treated similarly, except that E-selectin expression was induced by treating cells with TNF- $\alpha$  (10 ng/ml; R&D Systems) for 3 h, before a 1-h mAb incubation (4 h total). Dilutions, washes, and incubations occurred in HUVEC medium. All growth studies were performed at least three times in triplicate.

**Animal Studies.** Four- to six-week-old CB-17 SCID female mice, obtained from Taconic Farms and maintained in micro-isolator cages, received s.c. injections on the right flank of  $1 \times 10^7$  control HCT116-V, HCT116-13, or HCT116-35 cells. Tumors were allowed to establish for 10 days, reaching an average of 100 mm<sup>3</sup>, as determined by caliper measurement, and calculated by  $\pi/6 \times \text{length} \times \text{width} \times \text{height}$ . For each of the three tumor lines, animals were distributed into three groups and received PBS control ( $n = 4$ ), E-selectin-VC-MMAE conjugate at 0.134 mg/kg drug ( $\sim 3$  mg/kg mAb conjugate;  $n = 7$ ), or TIB191-VC-MMAE conjugate (0.134 mg/kg;  $n = 7$ ). Reagents were delivered by i.p. injection for four doses at 4-day intervals. Tumor volume was measured twice weekly, and clinical and mortality observations were performed daily according to Institutional Animal Care and Use Committee regulations.

## RESULTS

**Identification of E-Selectin as a Gene Specifically Up-Regulated in Human Prostate Cancer.** The goal of this study was to identify potential antibody therapeutic targets for the treatment of prostate cancer. Genes that encode these potential targets would ideally have

the following features: (a) up-regulation in prostate cancer; (b) little to no expression in normal nonprostate tissues to minimize undesirable side effects; and (c) cell surface localization for antibody accessibility. To identify such targets, 74 radical prostatectomy specimens representing localized prostate cancer with Gleason grades ranging from 6 to 9 and median prostate-specific antigen levels of 8.8 ng/ml (range, 3.1–90.4; Table 1) were processed for transcript profiling using the Eos Hu03 DNA expression array. Gene expression in these samples was compared with gene expression in over 200 normal tissue samples representing 43 different body tissues (the body atlas), including seven normal prostate samples (Fig. 1). Identified gene candidates were subjected to extensive bioinformatic analysis for gene identification, structural and functional classification, and identification of potential cell surface molecules. All probe sets on the Eos Hu03 DNA expression array were mapped to consensus gene clusters (Cluster and Alignment Tools, DoubleTwist) and the assembled human genome sequence (10). This allowed for robust gene identification and linking of the probe sets to public and internal gene annotation databases.

Surprisingly, one of the genes up-regulated in prostate cancer compared with normal prostate and normal body tissue was identified as E-selectin, a cell surface adhesion molecule long considered a vascular-specific antigen (National Center for Biotechnology Information reference sequence no. NM\_000450; GenBank M30640; Ref. 13). Fig. 1A shows E-selectin expression in the prostate cancer sam-

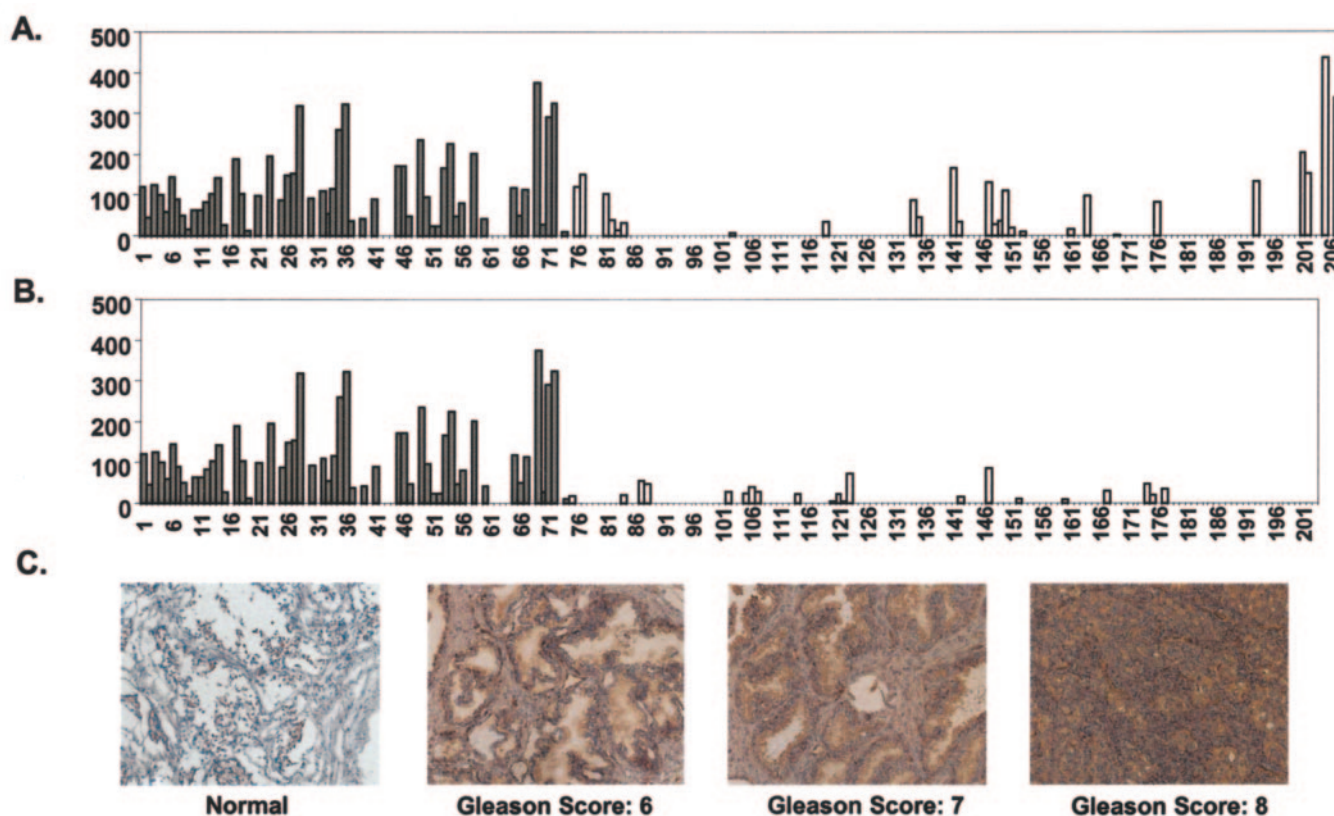


Fig. 1. E-selectin is preferentially up-regulated in prostate cancer. A, expression of E-selectin mRNA detected by Eos Hu03 microarray in prostate cancer samples and normal body tissues. AIU are shown on the Y axis. Samples, shown on the X axis, are: prostate cancer, 1–74; adipose tissue, 75–77; adrenal glands, 78–80; aorta, 81–83; appendix, 84–86; bladder, 87–89; bone marrow, 90–92; colonic epithelium, 93–95; cerebral cortex, 96–98; corpus callosum, 99–101; hypothalamus, 102–104; pituitary, 105–107; spinal cord, 108–110; thalamus, 111–113; colon, 114–116; esophagus, 117–119; epididymis, 120–122; heart, 123–125; kidney, 126–128; liver, 129–131; lung, 132–134; lymph node, 135–137; muscle, 138–140; larynx, 141–143; lip, 144–146; oral mucosa, 147–149; pharyngeal mucosa, 150–152; tongue, 153–155; pancreas, 156–158; prostate, 160–165; rectum, 166–168; retina, 169–171; salivary gland, 172–174; skin, 175–177; small intestine, 178–180; spleen, 181–183; stomach, 184–186; testis, 187–189; thymus, 190–192; parathyroid glands, 193–195; thyroid, 196–198; trachea, 199–201; coronary artery, 202–204; saphenous vein, 205–207. B, expression of E-selectin mRNA detected by Eos Hu03 microarray in prostate cancer, breast cancer, colon cancer, and testicular cancer. AIU are shown on the Y axis. Samples, shown on the X axis, are: prostate cancer, 1–74; breast cancer, 75–128; colon cancer, 129–177; testicular cancer, 178–203. C, immunostaining of normal prostate and prostate cancer. Normal and cancerous prostate sections were stained with the E-selectin mAb 5D11 as described in “Materials and Methods.” Depicted are sections from one normal prostate, two moderately differentiated malignant prostate, and one poorly differentiated malignant prostate (left to right). Gleason scores are indicated below each panel.



ples with respect to normal body tissues. These data show a 6-fold overexpression of the 85th percentile of E-selectin expression in prostate cancer (172 AIU) compared with the 85th percentile of normal tissue expression (29 AIU) and compared with the 85th percentile of normal prostate expression (26 AIU). Sixty-eight percent of the prostate cancer samples (*i.e.*, 50 of 74 cases) had AIU values above the 85th percentile for both normal prostate and normal tissue expression. No correlation was observed between Gleason score and E-selectin level. Other than prostate cancer, the tissue that exhibited the highest expression was saphenous vein (median expression of 338 AIU among three independent samples). It should be noted that female tissues (ovary, breast, endometrium, cervix, uterus, and vagina) were excluded from the analysis, because the objective was to identify molecules that, when targeted, would result in minimal side effects in prostate cancer patients. Subsequent expression analysis showed significant expression of E-selectin in cervix only (median expression of 244 AIU from five independent samples; data not shown). Interestingly, significant E-selectin overexpression was generally not observed in nonprostate malignant samples, including those from breast, colon, and testicular cancer (Fig. 1B).

To confirm up-regulation of E-selectin at the protein level, clinical prostate cancer sections were probed with a mAb (5D11) against human E-selectin. Preliminary experiments revealed that this antibody does not detect E-selectin in formalin-fixed paraffin-embedded tissue (data not shown), therefore, frozen tissue sections were used for immunohistochemical analysis; all stained sections were evaluated by an independent pathologist blinded to each sample. In concordance with the transcript profile, tissue-specific expression was detected in malignant prostate epithelium but not in normal prostate (Fig. 1C), consistent with the fact that E-selectin expression is inducible and is normally not present in resting tissues. Of 15 frozen prostate cancer sections analyzed, 14 stained positive for E-selectin. However, no correlation was observed between Gleason score and E-selectin level, in accordance with what was observed with our GeneChip array analysis (data not shown).

**Toxin-conjugated Anti-E-Selectin Antibodies Are Specific for E-Selectin-expressing Cells.** Our DNA microarray and immunohistochemical analysis revealed that E-selectin is overexpressed in prostate cancer epithelium relative to nearly all other tissues examined. To determine whether this relative difference in expression could be exploited for therapeutic use, we selectively targeted auristatin E, a small molecule toxin, to E-selectin-expressing cancer cells. An ADC was generated by attaching an average of eight molecules of auristatin E to the E-selectin-specific mAb 5D11. The conjugate, E-sel-VC-MMAE, was prepared such that each molecule of monomethyl auristatin E was attached to the mAb via a cathepsin B cleavable valine-citrulline dipeptide linker (6), allowing cleavage on mAb-antigen internalization to endosomes in cells (14, 15).

Initial *in vitro* studies used HUVECs that have been shown to up-regulate E-selectin in response to cytokines (16). For example, TNF- $\alpha$  can elicit surface expression of E-selectin within 4–6 h of treatment (Fig. 2A). To assess the potency and specificity of the E-sel-VC-MMAE ADC, HUVECs were exposed to various concentrations of ADC 4 h after TNF- $\alpha$  treatment. Dose-dependent cytotoxicity was observed in TNF- $\alpha$ -treated HUVECs, whereas untreated cells remained largely insensitive to the ADC (Fig. 2B). An irrelevant ADC, TIB191-VC-MMAE, was not cytotoxic to either treated or untreated cells. Treatment of either population with the unconjugated mAb, which has previously been demonstrated to neutralize E-selectin-mediated cell adhesion (17), had no effect on cell viability (data not shown). These results demonstrate that the anti-E-selectin ADC, unlike the unconjugated mAb, is selectively cytotoxic to E-selectin-expressing cells.

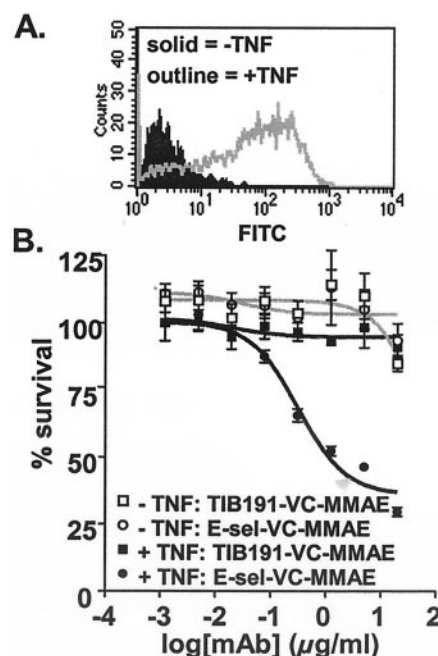


Fig. 2. Selective cytotoxicity of E-sel-VC-MMAE in HUVECs. A, HUVECs were treated with (*outline*) or without (*solid*) 10 ng/ml TNF- $\alpha$  for 4 h, and E-selectin up-regulation was measured by FACS using a FITC-conjugated E-selectin-specific mAb. B, E-sel-VC-MMAE decreases survival of E-selectin-expressing cells. HUVECs were treated with 10 ng/ml TNF- $\alpha$  for 3 h or left untreated before the addition of E-sel-VC-MMAE or TIB191-VC-MMAE ADC, at the indicated final concentrations, for 1 h. Cell viability was determined after 4 days, and survival was determined by subtracting background and normalizing absorbance values to an untreated control. Experiments were performed in triplicate, and curves were generated using GraphPad Prism graphing software.

**E-sel-VC-MMAE Toxicity Correlates with Antigen Surface Expression.** Close examination of the expression profile for E-selectin reveals that although E-selectin is overexpressed in prostate cancer epithelium, the level of expression varies widely between samples. This suggests that the level of surface E-selectin is likely to vary considerably among malignancies. Curiously, a wide spectrum of human cancer xenograft lines were negative for E-selectin, even in light of our immunohistochemical results clearly establishing E-selectin expression in transformed epithelium from human prostate cancer. It is not unusual for prostate-specific proteins to be absent in prostate cancer xenografts. Such lack of xenograft expression has been documented for the prostate-specific/enriched genes *PSA*, *PSCA*, and *Trp-p8* (18–20). Therefore, transfected xenograft cell lines were used for further analysis.

To explore the dependence of E-sel-VC-MMAE cytotoxicity on antigen density, PC3 prostate cancer, HCT116 colon carcinoma, and Calu6 lung cancer cells were transfected with a plasmid containing the full-length E-selectin open reading frame. Several stable lines were established by limiting dilution cloning and were assessed for constitutive E-selectin expression by flow cytometry. Comparison of numerous clones from PC3 and Calu6 revealed that clonal variability of E-selectin expression was very limited, with surface levels falling within 2-fold for each cell line (data not shown). The broadest range of expression was observed in the HCT116 clones, and five lines exhibiting varying levels of E-selectin surface expression (HCT116-13, -19, -35, -41, and -44) and a control cell line stably transfected with empty vector (HCT116-V) were chosen for further study based on this analysis (Fig. 3A). Two of these lines, HCT116-V and -35, were used to further show the specificity of the E-selectin-specific mAb 5D11 by immunofluorescence. As depicted in Fig. 3B, the antibody stains the high expressing line HCT116-35, whereas no

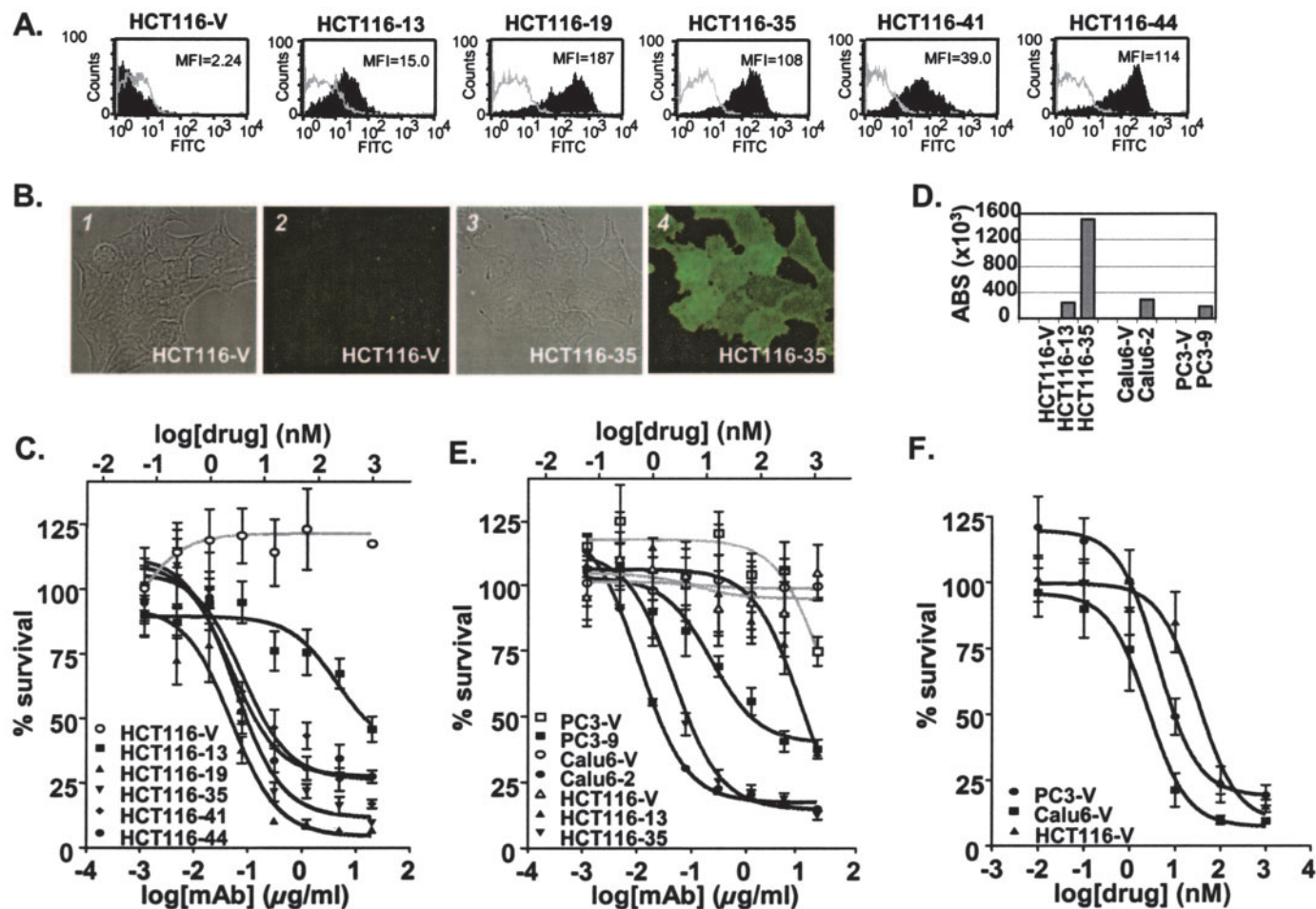


Fig. 3. Sensitivity to E-sel-VC-MMAE is cell line and antigen density dependent. In all cases, individual E-selectin clones are indicated by number, and mock stable lines are indicated by V. A, comparison of E-selectin-expressing HCT116 clones by flow cytometry. Individual HCT116 clones were stained with 10  $\mu\text{g/ml}$  isotype control (outline) or anti-E-selectin-FITC (solid) with the level of antigen expression determined by flow cytometry. B, specificity of anti-E-selectin antibody 5D11. HCT116-V or HCT116-35 cells were incubated with mAbs, and binding was detected using AlexaFluor-488-conjugated secondary antibody. Representative fields viewed in phase contrast in panels 1 and 3 are viewed by fluorescence microscopy in panels 2 and 4, respectively. C, cytotoxicity of E-sel-VC-MMAE in E-selectin-expressing HCT116 lines. HCT116 lines were challenged with various concentrations of E-sel-VC-MMAE for 1 h and assayed for viability 4 days later. Survival was determined as described in Fig. 2B. D, determination of relative antigen density in E-selectin-expressing cell lines. HCT116, Calu6, and PC3 cells expressing E-selectin were stained with anti-E-selectin-FITC and subjected to flow cytometry in parallel with similarly treated Quantum Simply Cellular (QSC) beads. Antibody binding sites (ABS) were determined by using the QSC beads as described in "Material and Methods." E, cytotoxicity of E-sel-VC-MMAE in various E-selectin-expressing cancer cell lines. E-selectin- or vector-transfected stable PC3, Calu6, and HCT116 lines were treated with the indicated concentrations of E-sel-VC-MMAE for 1 h and assessed for cell viability 4 days later. F, sensitivity of various cancer cell lines to auristatin E. PC3, Calu6, and HCT116 vector control lines were treated with free auristatin E for 1 h, and cell viability was assessed 4 days later.

fluorescence was detected in the HCT116-V control cell line. In addition, staining is only observed at the cell periphery, consistent with specific, cell surface expression of E-selectin.

As observed with TNF- $\alpha$ -treated HUVECs, treatment of each of the five E-selectin-expressing cell lines with E-sel-VC-MMAE resulted in dose-dependent cytotoxicity, whereas the vector control transfected cells (HCT116-V) remained unaffected (Fig. 3C). None of the cell lines were sensitive to the TIB191-VC-MMAE control mAb conjugate (data not shown). A strong correlation was observed between the level of surface E-selectin expression and susceptibility to the ADC (Fig. 3, A and C). However, significant differences in cytotoxicity were observed between HCT116-13 and HCT116-41 cells ( $\text{IC}_{50}$  of 4.5 and 0.082  $\mu\text{g/ml}$ , respectively), despite the relatively small difference in cell surface E-selectin (MFIs of 16 and 39, respectively). In fact, HCT116-41 is almost as susceptible to E-sel-VC-MMAE-mediated toxicity as clones that express much higher levels of surface antigen, such as HCT116-35 and HCT116-44 (MFIs of 107 and 114 and  $\text{IC}_{50}$  of 0.06 and 0.052  $\mu\text{g/ml}$ , respectively). These data indicate that ADC cytotoxicity increases with antigen density, and density

above a certain threshold results in particularly high sensitivity to the E-sel-VC-MMAE ADC.

**Dependence of E-sel-VC-MMAE Toxicity on Cell Type.** Having established the relationship between antigen density and cytotoxicity, we examined potential differences among individual cancer cell lines. For this study, stable E-selectin-expressing PC3 and Calu6 cell lines were used. Quantitative FACS was used to identify clonal lines derived from different cell types exhibiting similar levels of surface E-selectin expression (Fig. 3D). This revealed HCT116-13, Calu6-2 (Calu6-Esel clone 2), and PC3-9 (PC3-Esel clone 9) as clones with similar E-selectin cell surface expression.

E-selectin and vector control cell lines based on each cancer cell line were challenged with the E-sel-VC-MMAE *in vitro*. Despite similar levels of surface E-selectin, E-sel-VC-MMAE was most toxic to Calu6-2 and least toxic to HCT116-13 cells, with PC3-9 having intermediate sensitivity (Fig. 3E). This difference implies that susceptibility to E-sel-VC-MMAE is, at least in part, dictated by cell type.

To illuminate the basis for the differential sensitivity of these cell lines to an auristatin E-based conjugate, HCT116, PC3, and Calu6



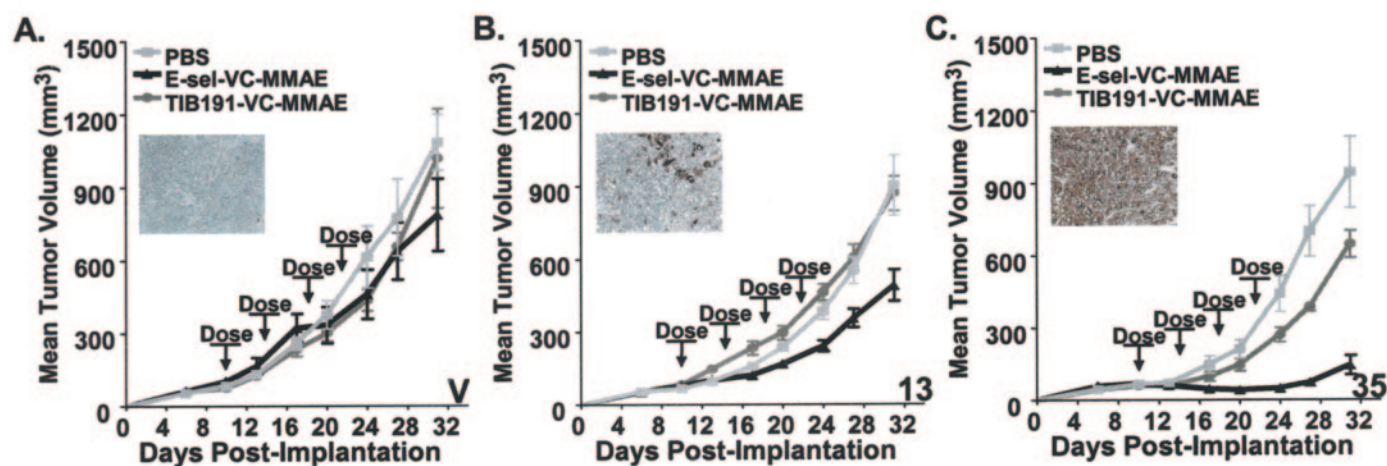


Fig. 4. Growth inhibition in an E-selectin-expressing xenograft model. CB-17 SCID mice bearing xenograft tumors derived from HCT116-V (A), HCT116-13 (B), or HCT116-35 (C) cells were dosed with 0.134 mg/kg E-sel-VC-MMAE, TIB191-VC-MMAE, or PBS 10 days after implantation and additionally on days 14, 18, and 22. Tumor size was assessed as described in "Materials and Methods." Insets depict typical staining of frozen, fixed xenograft sections from each clone with the anti-E-selectin mAb 5D11.

cells stably transfected with empty vector (HCT116-V, PC3-V, and Calu6-V, respectively) were exposed to various concentrations of free auristatin E in a manner similar to the ADC. The greatest sensitivity to auristatin E was observed with Calu6-V cells, followed by PC3-V and HCT116-V cells, demonstrating that sensitivity to free auristatin E also varies by cell type and is consistent with the differential effects of E-sel-VC-MMAE on these different cell types (Fig. 3F). Thus, it is likely that the potency of auristatin E-based ADC depends, in part, on the intrinsic sensitivity of a particular cell type to free auristatin E.

**Antitumor Activity of E-sel-VC-MMAE against E-Selectin-expressing Xenografts.** A murine xenograft model was used to assess whether E-sel-VC-MMAE was also selective for E-selectin-expressing cancer cells *in vivo*. CB-17 SCID mice bearing xenograft tumors derived from HCT116 cells expressing no, low, or high levels of E-selectin (HCT116-V, -13 and -35, respectively) were treated with E-sel-VC-MMAE, TIB191-VC-MMAE, or PBS. ADC (or PBS) was administered 10, 14, 18, and 22 days after implantation, and tumor size was monitored every 3 or 4 days for 31 days after implantation, or 3 weeks after initial dosing. ADC was administered at 0.134 mg/kg, which corresponds to less than one-third of the maximum tolerated dose (>0.3 mg/kg). Expression of E-selectin protein in frozen sections from each xenograft is shown (insets). E-selectin expression in the HCT116-13 and HCT116-35 xenografts are representative of low- and high-expressing human prostate cancer samples, respectively, based on staining of frozen prostate cancer sections (Fig. 1C; data not shown).

As depicted in Fig. 4B, growth of the low E-selectin-expressing tumor HCT116-13 was impeded by E-sel-VC-MMAE, relative to treatment with PBS or the TIB191-VC-MMAE-negative control conjugate ( $P = 0.0036$ ). In contrast, growth of the HCT116-V xenograft tumors was uninhibited by E-sel-VC-MMAE (Fig. 4A). Treatment of mice bearing high-expressing xenografts (HCT116-35) resulted in significant inhibition of tumor growth (Fig. 4C). Two weeks after treatment, E-sel-VC-MMAE-treated tumors were more than 85% smaller than their PBS-treated counterparts; a similar difference was observed 3 weeks after initial dosing. In all cases, the conjugates were well tolerated. No significant effects were observed in mice treated with the TIB191-VC-MMAE-negative control, confirming that tumor reduction depended on targeting of the toxin with the E-selectin antibody. These statistically significant results ( $P = 0.0002$ ) correlate well with our *in vitro* data, suggesting that E-sel-VC-MMAE is an

effective anticancer agent against E-selectin-positive xenograft tumors in mice. This observation is particularly compelling given that the background cell line (HCT116) exhibited the lowest sensitivity to auristatin E *in vitro* (Fig. 3F).

## DISCUSSION

The lack of specificity displayed by most current cancer treatments often results in significant toxicity to noncancerous tissues. As a result, the identification of cancer-specific antigens for use as therapeutic targets has proven of great clinical interest. Only a subset of these may be required for cancer cell survival or motility, including HER2 in breast cancer epithelium, CD20 in lymphocytic B-cells, and Bcr-Abl in chronic myelogenous leukemia (21, 22).

The development of genomics technology has made available the rapid and comprehensive screening of diseased tissues for specifically up-regulated target molecules suitable for antibody targeting. Our proprietary GeneChip array, Eos Hu03, which represents over 92% coverage of the human genome, combined with an extensive library of prostate cancer samples and a human body atlas, provides a powerful platform for the identification of cancer-enriched mRNAs. Using these genomics capabilities, we identified E-selectin as a novel prostate cancer-enriched antigen. This finding was surprising given that E-selectin expression had previously been thought to be confined to activated endothelium. Accordingly, we were not able to detect E-selectin expression in any of 57 xenograft cell lines initially tested, including the prostate cancer cell lines DU145, PC3, or LNCaP. Furthermore, no E-selectin expression was detected when this analysis was expanded to include the prostate cancer xenografts LuCaP, CWR22, CWR22R, and RPWE2. However, E-selectin expression has been associated with tumor angiogenesis and metastasis in a variety of cancers (23). Moreover, E-selectin induction is increased in hypoxic endothelium and is generally thought to be completely dependent on the paracrine activity of inflammatory cytokines (24, 25). These observations argue that E-selectin expression in prostate cancer is likely the result of complex interactions within the tumor microenvironment that are not easily reproduced in cell culture or mouse xenograft models. As a result, this study has relied largely on transfected E-selectin-expressing cancer cell lines for both *in vitro* and *in vivo* studies. These cell lines expressed E-selectin across a similar range of expression observed in our radical prostatectomy specimens.

In accordance with other studies, we found that an unconjugated anti-E-selectin mAb (5D11) that blocks its adhesion properties to leukocytes does not retard the growth of E-selectin-expressing cells in culture (17, 26, 27). Anti-E-selectin mAbs can, however, facilitate the entry of immunoliposomes or other mAb conjugates into cells *in vitro* (28–30). One method to use highly selective proteins for cancer therapy is to exploit these molecules for targeted delivery of a toxic agent. Toxins that have successfully been used include both small molecule agents, such as calicheamicin, and radionuclides, such as  $^{111}\text{In}$  or  $^{90}\text{Y}$  (31–33). These agents can be very effective when conjugated to a mAb that directs them to a cancer cell-specific surface antigen. Examples of clinically approved anticancer ADCs include Mylotarg and Zevalin, for acute myeloid leukemia and refractory non-Hodgkin's lymphoma, respectively (31–33).

Recently, a mAb directed against PSCA and conjugated to the maytansinoid toxin DM1 was found to inhibit tumor growth in a xenograft model (34). In that study, DM1 was conjugated to an anti-PSCA antibody via a disulfide linkage designed to remain intact in the circulation, dissolving only within the reductive environment of the cell. However, in at least two studies using DM1 conjugates, certain nonspecific effects have been observed (34, 35), suggesting that a portion of these conjugates may disintegrate prematurely. To circumvent this potential problem, we compared a number of linker systems for stability and selectivity. For example, a hydrazone linker, designed to remain intact in the circulation but to be unstable at intracellular pH, was found to be relatively unstable in *in vitro* and *in vivo* models, resulting in high nonspecific toxicity and low selectivity. We have, therefore, used a peptide linker cleavable by the proteolytic enzyme cathepsin B, which is elevated in a wide range of malignancies (36, 37). This linker is labile only on internalization to compartments containing cathepsin B, such as endosomes or lysosomes, resulting in a 20- to 50-fold greater selectivity than the aforementioned hydrazone linker (data not shown; Ref. 6). We have placed this linker between a highly specific mAb to human E-selectin and auristatin E, an inhibitor of microtubule polymerization several orders of magnitude more cytotoxic than many commonly used chemotherapeutics (7, 38). This combination of a tumor-targeting antibody, an enzyme cleavable linker, and a potent mediator of apoptosis in rapidly dividing cells has resulted in a novel, highly selective, and efficacious anticancer agent in preclinical models.

Our findings demonstrate that an E-selectin mAb conjugated to auristatin E is a potent and specific cytotoxic agent against E-selectin-expressing cancer cells. Importantly, this ADC, E-sel-VC-MMAE, was able to significantly inhibit tumor cell proliferation both *in vitro* and *in vivo* in a mouse xenograft model. A distinguishing feature of E-selectin, relative to other ADC targets described thus far, is that it is also highly expressed in activated endothelium. Using an E-selectin-specific ADC may have the dual effect of targeting the cancer epithelium itself, as well as the neovasculature supplying blood to the prostate tumor (23, 30). This hypothesis was not testable in the current experimental paradigm because the mAb was specific to human E-selectin and, therefore, would not target any murine-derived neovasculature sustaining tumor growth. Thus, the efficacy of the ADC in the current *in vivo* model must directly target the prostate carcinoma cells. A potential side effect of an ADC targeting antigens expressed on nascent vasculature, such as that involved in wound healing, cannot be ruled out, although even in this situation differential levels of expression between tumor cells and normal tissues may provide a therapeutic window. In this regard, it is worthy of note that some venous tissues, particularly saphenous vein, expressed high levels of E-selectin mRNA. Whether this would translate into significant toxic side effects could not be tested in the xenograft model because the mAb did not recognize mouse E-selectin. Consequently, other studies

in nonhuman primates will be needed to address tissue-specific toxicity.

The data presented herein indicate that an ADC approach may be of use in the treatment of prostate cancer. Although ADCs may be useful against many proliferative diseases, our data suggest that sensitivity to auristatin E among different cancer cell lines varies by as much as 10-fold, thus the effectiveness of a particular ADC may vary between malignancies. Moreover, our data indicate that antigen density contributes greatly to the efficacy of ADCs both *in vitro* and *in vivo*. This is in accord with studies demonstrating that the E-selectin internalization is proportional to its cell surface density, which, in endothelial cells, reaches a maximum 4–6 h after stimulation (13, 39, 40). In addition, we show that a threshold of antigen density must be reached to achieve high levels of cytotoxicity. This observation is significant because it suggests that auristatin E-conjugated mAbs preferentially kill cells that express high levels of a given antigen, while sparing normal cells that may express lower, physiological levels of antigen. Thus, our data demonstrate a potential selective anticancer strategy that may tolerate minimal target expression in normal body tissues.

Antibody-based therapeutics have proven successful against many cancers. The high affinity and unparalleled specificity of antibodies can prove to be a significant advantage over equivalent small molecules. Moreover, unlike small molecule inhibitors, ADCs need not rely solely on the function of the antigen in the maintenance or progression of cancer. Furthermore, efficacy can potentially be enhanced by combining immunotherapy with chemotherapy (41). The present proof of principle study demonstrates potential use for an auristatin E-E-selectin mAb conjugate in prostate cancer. Similar conjugates could be of appreciable use against a variety of proliferative diseases in which the therapeutic intent does not rely completely on mechanistic interruption, but on targeted destruction of the disease-causing cell.

## ACKNOWLEDGMENTS

We thank Keith Wilson for critical reading of this manuscript and helpful discussions and Therese Anderson, Pauline Wales, and Vicky Dulai for assistance with cell culture and maintenance.

## REFERENCES

- Critz, F. A. The Facts About Prostate Cancer. Vol. 2002: Radiotherapy Clinics of Georgia. Atlanta, Georgia, 2002.
- Bevilacqua, M. P., Stengelin, S., Gimbrone, M. A., Jr., and Seed, B. Endothelial leukocyte adhesion molecule 1: an inducible receptor for neutrophils related to complement regulatory proteins and lectins. *Science (Wash. DC)*, *243*: 1160–1165, 1989.
- Pober, J. S., Kluger, M. S., and Schechner, J. S. Human endothelial cell presentation of antigen and the homing of memory/effector T cells to skin. *Ann. N. Y. Acad. Sci.*, *941*: 12–25, 2001.
- Rosen, S. D. Cell surface lectins in the immune system. *Semin. Immunol.*, *5*: 237–247, 1993.
- Phillips, M. L., Nudelman, E., Gaeta, F. C., Perez, M., Singhal, A. K., Hakomori, S., and Paulson, J. C. ELAM-1 mediates cell adhesion by recognition of a carbohydrate ligand, sialyl-Lex. *Science (Wash. DC)*, *250*: 1130–1132, 1990.
- Doronina, S., Toki, B., Torgov, M., Mendelsohn, B., Cervent, C., Chace, D., DeBlanc, R., Gearing, R., Bovee, T., Siegall, C., Francisco, J., Wahl, A., Meyer, D., and Senter, P. Development of potent monoclonal antibody auristatin conjugates for cancer therapy. *Nat. Biotechnol.*, *21*: 778–784, 2003.
- Pettit, G. R., Sriangam, J. K., Barkoczy, J., Williams, M. D., Boyd, M. R., Hamel, E., Pettit, R. K., Hogan, F., Bai, R., Chapuis, J. C., McAllister, S. C., and Schmidt, J. M. Antineoplastic agents 365. Dolastatin 10 SAR probes. *Anticancer Drug Des.*, *13*: 243–277, 1998.
- Mohammad, R. M., Varterasian, M. L., Almatchy, V. P., Hannoudi, G. N., Pettit, G. R., and Al-Katib, A. Successful treatment of human chronic lymphocytic leukemia xenografts with combination biological agents auristatin PE and bryostatins 1. *Clin. Cancer Res.*, *4*: 1337–1343, 1998.
- Henshall, S., Afar, D., Hiller, J., Horvath, L., Quinn, D., Rasiah, K., Gish, K., Willhite, D., Kench, J., Gardiner-Garden, M., Stricker, P., Scher, H., Grygiel, J., Agus, D. D., M., and Sutherland, R. Survival analysis of genome-wide gene expression profiles of prostate cancers identifies new prognostic targets of disease relapse. *Cancer Res.*, *63*: 4196–4203, 2003.

10. Platzer, P., Upender, M. B., Wilson, K., Willis, J., Lutterbaugh, J., Nosrati, A., Willson, J. K., Mack, D., Ried, T., and Markowitz, S. Silence of chromosomal amplifications in colon cancer. *Cancer Res.*, *62*: 1134–1138, 2002.
11. Brockhoff, G., Hofstaedter, F., and Kneuchel, R. Flow cytometric detection and quantitation of the epidermal growth factor receptor in comparison to Scatchard analysis in human bladder carcinoma cell lines. *Cytometry*, *17*: 75–83, 1994.
12. Islam, D., Wretling, B., Lindberg, A. A., and Christensson, B. Changes in the peripheral blood T-cell receptor V  $\beta$  repertoire in vivo and in vitro during shigellosis. *Infect. Immun.*, *64*: 1391–1399, 1996.
13. Kluger, M. S., Johnson, D. R., and Pober, J. S. Mechanism of sustained E-selectin expression in cultured human dermal microvascular endothelial cells. *J. Immunol.*, *158*: 887–896, 1997.
14. Driessen, C., Lennon-Dumenil, A. M., and Ploegh, H. L. Individual cathepsins degrade immune complexes internalized by antigen-presenting cells via Fc $\gamma$  receptors. *Eur. J. Immunol.*, *31*: 1592–1601, 2001.
15. Walker, M. A., Dubowchik, G. M., Hofstead, S. J., Trail, P. A., and Firestone, R. A. Synthesis of an immunconjugate of camptothecin. *Bioorg. Med. Chem. Lett.*, *12*: 217–219, 2002.
16. Montgomery, K. F., Osborn, L., Hession, C., Tizard, R., Goff, D., Vassallo, C., Tarr, P. I., Bomszyk, K., Lobb, R., Harlan, J. M., and et al. Activation of endothelial-leukocyte adhesion molecule 1 (ELAM-1) gene transcription. *Proc. Natl. Acad. Sci. USA*, *88*: 6523–6527, 1991.
17. Pigott, R., Needham, L. A., Edwards, R. M., Walker, C., and Power, C. Structural and functional studies of the endothelial activation antigen endothelial leucocyte adhesion molecule-1 using a panel of monoclonal antibodies. *J. Immunol.*, *147*: 130–135, 1991.
18. Saffran, D. C., Raitano, A. B., Hubert, R. S., Witte, O. N., Reiter, R. E., and Jakobovits, A. Anti-PSCA mAbs inhibit tumor growth and metastasis formation and prolong the survival of mice bearing human prostate cancer xenografts. *Proc. Natl. Acad. Sci. USA*, *98*: 2658–2663, 2001.
19. Tsavaler, L., Shaper, M. H., Morkowski, S., and Laus, R. Trp-p8, a novel prostate-specific gene, is up-regulated in prostate cancer and other malignancies and shares high homology with transient receptor potential calcium channel proteins. *Cancer Res.*, *61*: 3760–3769, 2001.
20. Navone, N. M., Logothetis, C. J., von Eschenbach, A. C., and Troncoso, P. Model systems of prostate cancer: uses and limitations. *Cancer Metastasis Rev.*, *17*: 361–371, 1998.
21. Carter, P. Improving the efficacy of antibody-based cancer therapies. *Nat. Rev. Cancer*, *1*: 118–129, 2001.
22. Mauro, M. J., O'Dwyer, M., Heinrich, M. C., and Druker, B. J. STI571: a paradigm of new agents for cancer therapeutics. *J. Clin. Oncol.*, *20*: 325–334, 2002.
23. Laferriere, J., Houle, F., and Huot, J. Regulation of the metastatic process by E-selectin and stress-activated protein kinase-2/p38. *Ann. N. Y. Acad. Sci.*, *973*: 562–572, 2002.
24. Zund, G., Nelson, D. P., Neufeld, E. J., Dzus, A. L., Bischoff, J., Mayer, J. E., and Colgan, S. P. Hypoxia enhances stimulus-dependent induction of E-selectin on aortic endothelial cells. *Proc. Natl. Acad. Sci. USA*, *93*: 7075–7080, 1996.
25. Ley, K. Pathways and bottlenecks in the web of inflammatory adhesion molecules and chemoattractants. *Immunol. Res.*, *24*: 87–95, 2001.
26. Benjamin, C., Douglas, I., Chi-Rosso, G., Luhowskyj, S., Rosa, M., Newman, B., Osborn, L., Vassallo, C., Hession, C., Goelz, S., et al. A blocking monoclonal antibody to endothelial-leukocyte adhesion molecule-1 (ELAM1). *Biochem. Biophys. Res. Commun.*, *171*: 348–353, 1990.
27. Berg, E. L., Fromm, C., Melrose, J., and Tsurushita, N. Antibodies cross-reactive with E- and P-selectin block both E- and P-selectin functions. *Blood*, *85*: 31–37, 1995.
28. Everts, M., Kok, R. J., Asgeirsdottir, S. A., Melgert, B. N., Moolenaar, T. J., Koning, G. A., van Luyn, M. J., Meijer, D. K., and Molema, G. Selective intracellular delivery of dexamethasone into activated endothelial cells using an E-selectin-directed immunconjugate. *J. Immunol.*, *168*: 883–889, 2002.
29. Kessner, S., Krause, A., Rothe, U., and Bendas, G. Investigation of the cellular uptake of E-selectin-targeted immunoliposomes by activated human endothelial cells. *Biochim. Biophys. Acta*, *1514*: 177–190, 2001.
30. Spragg, D. D., Alford, D. R., Greferath, R., Larsen, C. E., Lee, K. D., Gurtner, G. C., Cybulsky, M. I., Tosi, P. F., Nicolau, C., and Gimbrone, M. A., Jr. Immunotargeting of liposomes to activated vascular endothelial cells: a strategy for site-selective delivery in the cardiovascular system. *Proc. Natl. Acad. Sci. USA*, *94*: 8795–8800, 1997.
31. van Der Velden, V. H., te Marvelde, J. G., Hoogveen, P. G., Bernstein, I. D., Houtsmuller, A. B., Berger, M. S., and van Dongen, J. J. Targeting of the CD33-calicheamicin immunconjugate Mylotarg (CMA-676) in acute myeloid leukemia: in vivo and in vitro saturation and internalization by leukemic and normal myeloid cells. *Blood*, *97*: 3197–3204, 2001.
32. Wiseman, G. A., Gordon, L. I., Multani, P. S., Witzig, T. E., Spies, S., Bartlett, N. L., Schilder, R. J., Murray, J. L., Saleh, M., Allen, R. S., Grillo-Lopez, A. J., and White, C. A. Ibritumomab tiuxetan radioimmunotherapy for patients with relapsed or refractory non-Hodgkin lymphoma and mild thrombocytopenia: a phase II multicenter trial. *Blood*, *99*: 4336–4342, 2002.
33. Witzig, T. E., Gordon, L. I., Cabanillas, F., Czuczman, M. S., Emmanouilides, C., Joyce, R., Pohlman, B. L., Bartlett, N. L., Wiseman, G. A., Padre, N., Grillo-Lopez, A. J., Multani, P., and White, C. A. Randomized controlled trial of yttrium-90-labeled ibritumomab tiuxetan radioimmunotherapy versus rituximab immunotherapy for patients with relapsed or refractory low-grade, follicular, or transformed B-cell non-Hodgkin's lymphoma. *J. Clin. Oncol.*, *20*: 2453–2463, 2002.
34. Ross, S., Spencer, S. D., Holcomb, I., Tan, C., Hongo, J., Devaux, B., Rangell, L., Keller, G. A., Schow, P., Steeves, R. M., Lutz, R. J., Frantz, G., Hillan, K., Peale, F., Tobin, P., Eberhard, D., Rubin, M. A., Lasky, L. A., and Koeppen, H. Prostate stem cell antigen as therapy target: tissue expression and *in vivo* efficacy of an immunconjugate. *Cancer Res.*, *62*: 2546–2553, 2002.
35. Liu, C., Tadayoni, B. M., Bourret, L. A., Mattocks, K. M., Derr, S. M., Widdison, W. C., Kedersha, N. L., Ariniello, P. D., Goldmacher, V. S., Lambert, J. M., Blattler, W. A., and Chari, R. V. Eradication of large colon tumor xenografts by targeted delivery of maytansinoids. *Proc. Natl. Acad. Sci. USA*, *93*: 8618–8623, 1996.
36. Yan, S., Sameni, M., and Sloane, B. F. Cathepsin B and human tumor progression. *Biol. Chem.*, *379*: 113–123, 1998.
37. Sinha, A. A., Jamuar, M. P., Wilson, M. J., Rozhin, J., and Sloane, B. F. Plasma membrane association of cathepsin B in human prostate cancer: biochemical and immunogold electron microscopic analysis. *Prostate*, *49*: 172–184, 2001.
38. Mohammad, R. M., Limvarapuss, C., Wall, N. R., Hamdy, N., Beck, F. W., Pettit, G. R., and Al-Katib, A. A new tubulin polymerization inhibitor, auristatin PE, induces tumor regression in a human Waldenstrom's macroglobulinemia xenograft model. *Int. J. Oncol.*, *15*: 367–372, 1999.
39. Kluger, M. S., Shiao, S. L., Bothwell, A. L., and Pober, J. S. Cutting edge: internalization of transduced E-selectin by cultured human endothelial cells—comparison of dermal microvascular and umbilical vein cells and identification of a phosphoserine-type di-leucine motif. *J. Immunol.*, *168*: 2091–2095, 2002.
40. Chuang, P. I., Young, B. A., Thiagarajan, R. R., Cornejo, C., Winn, R. K., and Harlan, J. M. Cytoplasmic domain of E-selectin contains a non-tyrosine endocytosis signal. *J. Biol. Chem.*, *272*: 24813–24818, 1997.
41. Thomssen, C. Trials of new combinations of Herceptin in metastatic breast cancer. *Anticancer Drugs*, *12* (Suppl 4): S19–S25, 2001.